JOURNAL OF APPLIED ELECTROCHEMISTRY 17 (1987) 303–314

*Characteristics and properties of electrodeposited chromium from aqueous solutions**

M. McCORMICK, S. J. DOBSON

Department of Electronic and Electrical Engineering, Sheffield University, Mappin Street, Sheffield S1 3JD, UK

Received 10 April 1986; revised 17 September 1986

The characteristics and properties of chromium deposited from sulphate-catalysed chromic acid solutions of varying composition over both a current density and temperature range have been examined. An attempt to interpret the mechanical test results on the basis of inherent crack incidence and crack length within the deposit has also been presented.

Comparisons between laboratory and commercial platings have established the viability of extrapolating the laboratory results, enabling test gun tube performance to be related to the various coating structures produced in the 120 mm barrel by the varying current density conditions experienced. These current density variations have been predicted using the boundary element numerical method which demonstrates the inherent problems associated with gun tube geometry.

1. Introduction

Although the deposit mechanisms of hard chromium plating are incompletely understood, the production of sound, high-quality coatings from catalysed chromic acid solutions has been thoroughly researched [1, 2] and is consistently practised. Most engineering coatings are produced from baths catalysed by the sulphate acid radical with an accepted optimum ratio of chromic to sulphuric acid of 100 : 1. Alternative catalysts have been investigated but not adopted [3]; however, additives are commonly added to the standard electrolyte to enhance some aspect of either the process performance or deposit characteristics. The role of the catalyst is still incompletely understood and a review by Hoare [4] presents several differing schools of thought as well as a proposed mechanistic role for the sulphate radical. However, at present, no completely satisfactory explanation exists for the cathodic process during electrodeposition. This is not altogether surprising considering the number of chromic complexes [5–7] present, the species involved and the competing reactions. Galvanostatic and potentiostatic polarization curves have been usefully employed in elucidating some of the effects concomitant with the addition of catalysts [4, 7–9].

Further investigations using linear sweep and cyclic voltammetry on a 250 g l^{-1} CrO_3, sulphate-catalysed electrolyte using chromium, nickel, copper and vitreous carbon cathodes have also recently been reported by Lin-Cai and Pletcher [10, 11]. Their results confirm the basic reactions occurring at successively more negative potentials in chromium electrolytes and explain other features such as the effect of the sulphate ion concentration on the limiting current of the Cr(VI) to Cr(III) reduction, the effect of the substrate on the potential at which the initial passivating film is dissolved and, finally, the conditions necessary for the nucleation of the metallic phase.

Until recently [12] perhaps the most useful addition to the standard electrolyte was considered to be a complex fluoride which improves both process efficiency and deposit hardness [13]. The major disadvantage of fluoride additions is that non-plated areas are etched, and for appli-

* This paper was presented at a workshop on the electrodeposition of refractory metals, held at Imperial College, London, in July 1985.

0021–891X/87 $03.00 + .12 © 1987 Chapman and Hall Ltd.

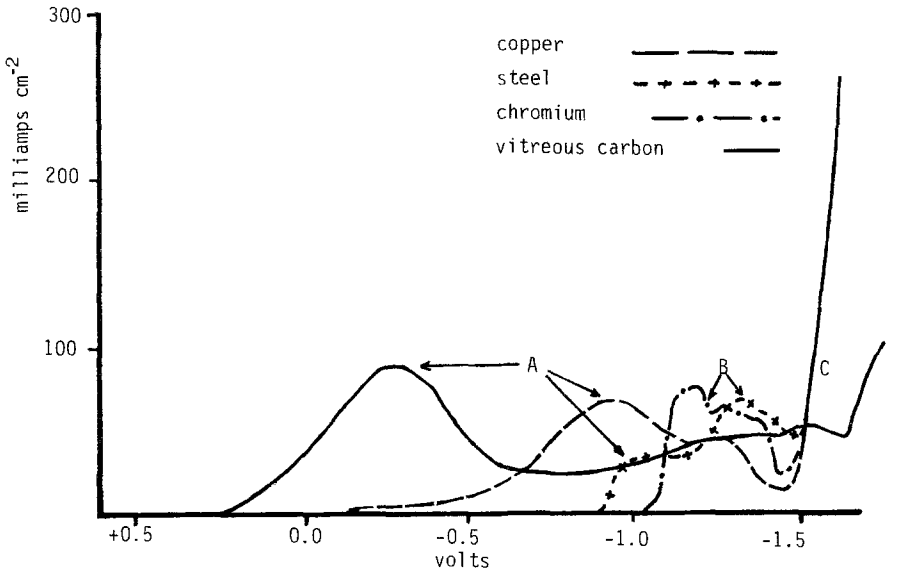

Fig. 1. Linear potential sweep curves on copper, steel, chromium and vitreous carbon for a standard solution.

cations such as the plating of gun tubes they are consequently unsuitable. Although high efficiency, non-etching solutions are now available [12, 14], these have not been considered and this paper concentrates on chromium coatings from basic sulphate-catalysed solutions.

The typical performance of aqueous sulphate-catalysed hexavalent chromium electrolytes is illustrated in Fig. 1, where linear sweep current–potential curves are shown for four substrates used in a standard 100:1 ratio CrO_3/H_2SO_4 (450 : 4.5 g l^{-1}) electrolyte. Each curve shows the distinctive regions associated with chromium electrolytes as the potential at the working electrode is made more cathodic. The initial reaction (A) is that associated with the Cr(VI) to Cr(III) reduction and is followed by a passive region and a second peak (B) due to hydrogen evolution. As reported by Saiddington and Hoey [15] this peak is followed by a second passive region before the onset of chromium plating together with renewed Cr(VI) to Cr reduction and hydrogen evolution (C).

As can be seen from Fig. 2, the potential at

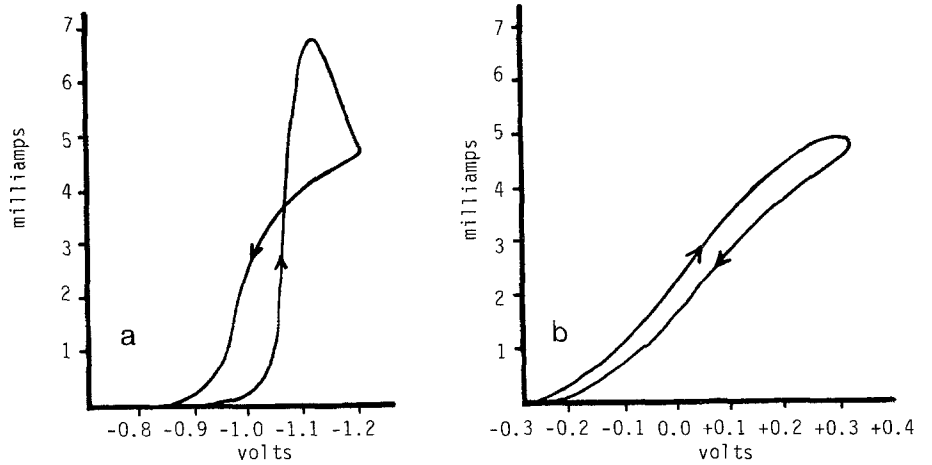

Fig. 2. Cyclic voltammograms for a 450 g l^{-1} CrO_3 + 4.5 g l^{-1} H_2SO_4 solution (a) copper and (b) vitreous carbon. Potential sweep rate, 20 mV s^{-1}.

which the Cr(VI) to Cr(III) reduction occurs is highly substrate-dependent, occurring at approximately -0.24 V on vitreous carbon (in the absence of an oxide film on the cathode surface) and at successively more cathodic potentials on copper (-0.90 V), steel (-1.0 V) and chromium (-1.15 V), reflecting the relative strength of the oxide film formed on immersion of the substrate. The existence of the oxide film and the role of sulphate has been fully dealt with by Lin-Cai and Pletcher [10, 11] who obtained similar curves to those shown in Figs 1 and 2. In Fig. 2, cyclic voltammograms are shown for chromium and vitreous carbon substrates where the sweep is reversed at a potential slightly more cathodic than the Cr(VI)to Cr(III) reduction peak (A). It can be seen that chromium, like all other metal substrates examined, exhibits a 'nucleation loop' which has been shown to be due to the nucleation and growth of holes in the oxide film on the metal substrates [10]. This phenomenon does not occur on vitreous carbon since no oxide film is formed and Cr(VI) to Cr(III) reduction can occur at a potential closer to that expected for the Cr(VI)/Cr(III) couple.

Also in Fig. 2, it can be seen that hydrogen evolution occurs at approximately -1.30 V, independent of substrate material, and the reactions which finally lead to reduction of Cr(VI) to Cr, Cr(VI) to Cr(III) and further hydrogen production, occur at identical potentials for the metal substates concerned. Only the vitreous carbon shows any variation, this being explained by the increased energy required to cause nucleation on the nonmetallic structure.

It is common knowledge that the properties and structural characteristics of electrodeposited chromium coatings are affected by both process conditions and solution additives. However, although a number of technical papers [16, 17] have been devoted to this topic, no coherent, wide-ranging study has been carried out which fully categorizes chromium coating characteristics either over the normal operating range or in solutions with varying sulphate ratios operating at various temperatures. Also as the most desirable properties required for gun tube applications are unknown, a programme of work to establish a coatings information base to be used in conjunction with results from a test firing programme is a sensible approach.

In gun tube geometries a range of current density conditions exist, especially in the rifled section and at the barrel–chamber transition. As coating structure is sensitive to current density this prevents homogeneous deposits being produced. Therefore, in practical systems the anode–cathode geometry and operating parameters must, where possible, be contrived to produce the most desirable coating conditions in specific sensitive areas. To correlate accurately the structure and properties to current density conditions a number of test fixtures have been designed, in which this parameter is accurately controlled. This allows current to be accurately related to cathode surface conditions during the production of coatings for examination and test.

The present work was undertaken in an effort to upgrade the standard chromium process for gun tube applications, and therefore correlation of results obtained from pilot plant scale tests and those industrially produced in a nominal 100:1 CrO_3/H_2SO_4 bath are considered.

2. Experimental details

2.1. *General procedures*

All test platings for microscopic examination were carried out in an H-cell in which the cathode was accommodated in a specially designed jig which produced a predominantly uniform current density over the area to be plated. This arrangement has been previously reported [18] and conditions at the cathode surface are those consistent with an unagitated bath, i.e. electrolyte flow and mixing is induced by the hydrogen liberated from the cathode surface. Electrolysis conditions were standardized, each solution being subjected to a plating current of 1 A $h l^{-1}$. The test cell volume was 1.5 litres and solution temperature was controlled to within $\pm 1^\circ$ C in all test fixtures.

In all tests a Farnell constant-current power supply was used. Substrate materials chosen were 18/8 stainless steel for the micrographic samples, a low carbon strip steel for adhesion and stress measurements and copper tube for the tensile samples. All samples were mechanically

Table 1. Current efficiency and deposit rate for electrodeposited chromium with variation of current density and $CrO_3 : H_2SO_4$ ratio. Process temperature, 55° C

Current density ($A\,dm^{-2}$)	Current efficiency (%)					Deposit rate ($\mu m\,h^{-1}$)				
	80:1	90:1	100:1	110:1	125:1	80:1	90:1	100:1	110:1	125:1
20	12.0	11.5	11.7	10.3	0.5	10.1	9.3	9.4	9.3	8.0
30	14.3	13.9	14.0	14.0	12.4	18.4	16.1	17.1	17.3	15.5
50	18.4	17.1	17.4	16.8	16.1	39.8	37.5	36.7	34.0	31.0
75	18.9	18.1	17.5	17.1	16.4	54.6	52.5	54.3	51.8	50.5

polished using 600 grade emery or a fine wire wool and Brasso, with the exception of some adhesion test substrates and 30 mm liners which were electropolished in a phosphoric–sulphuric–chromic solution. The basic surface treatment prior to plating was an acetone degrease and then electrolytic cleaning (anodic) in 10% NaOH, followed by a thorough rinse in deionized water. For the steel specimens a standard 'free' corrosion time of 2 min was allowed prior to plating. A reverse etch prior to plating was only used when plating gun tubes.

For test purposes chromium coatings were produced from solutions containing $250\,g\,l^{-1}$ chromic acid with sulphate ratios varying from 80:1 to 125:1 at current densities of 20, 30, 50 and $75\,A\,dm^{-2}$ and over a temperature range 45–85° C. Reagent grade chemicals were used and solutions were prepared with deionized water. At the present time gun tubes in the UK are coated in solutions operating at 55° C, and to minimize data complexity only results obtained at this temperature are presented.

2.2. *Structural characteristics of the coating*

The chromium deposits produced in laboratory tests were consistently sound, bright and non-nodular even though coatings at $75\,A\,dm^{-2}$ were produced. The plating rate and cathode current efficiencies for solutions of various sulphate ratios are shown in Table 1.

Transverse sections of the plated specimens show a variation in crack incidence with both sulphate ratio and current density as illustrated in Fig. 3. Micrographs corresponding to coatings produced at $20\,A\,dm^{-2}$ for the various solutions are shown in Fig. 4 from which it is apparent that crack length is a function of sulphate ratio. In Fig. 5, the effect of current density on crack length is illustrated showing that in solutions with chromic sulphuric acid ratios

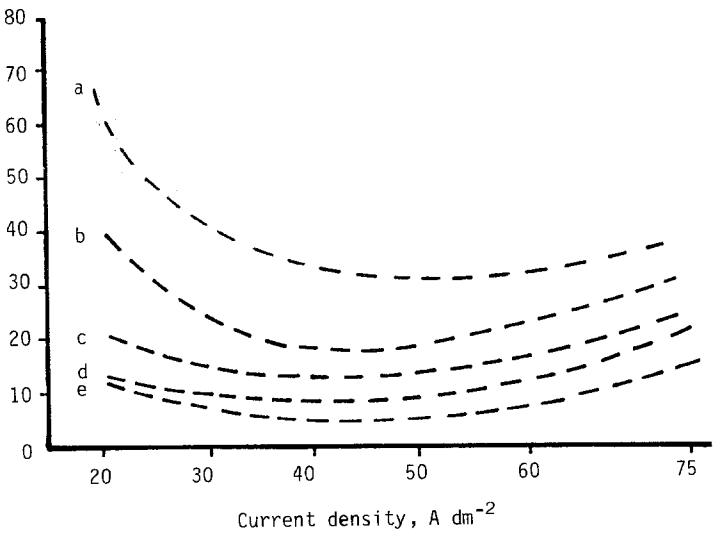

Fig. 3. Crack incidence per $20\,000\,\mu m^2$ versus current density for various sulphate ratios: (a) 80:1; (b) 90:1; (c) 100:1; (d) 110:1 (e) 125:1.

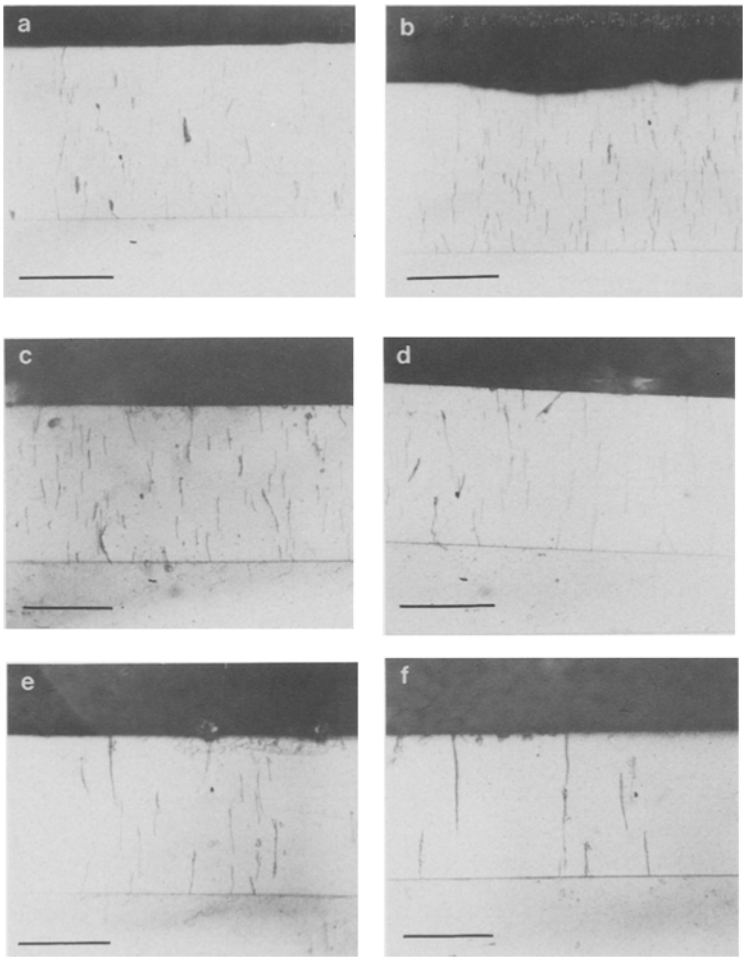

Fig. 4. Transverse sections of chromium deposits produced at 20 A dm^{-2} from solutions with various sulphate ratios (six photos). Chromic to sulphuric acid ratios: (a) 80 : 1; (b) 90 : 1; (c) 100 : 1; (d) 110 : 1; (e) 125 : 1; (f) 150 : 1. Scale bars: 57 μm.

between 80 : 1 to 110 : 1 there is a rapid decrease in crack length at very low current densities. Also in these solutions the crack length appears to increase slightly between 30–50 A dm^{-2}, while crack incidence and crack length are sensitive for current densities less than 30 A dm^{-2}. Below 20 A dm^{-2} the crack intensity increases rapidly while the crack length decreases. This is illustrated in Fig. 6 and these conditions are to be expected in the grooves of gun tubes plated in the commercial plating facility where an average current density of 20 A dm^{-2} is used.

The results presented are taken from four separate transverse sections, each count being taken over a length of 200 μm. The results are then normalized to a coating thickness of 100 μm, corresponding to the crack incidence over an area of 20 000 μm^2, prior to averaging.

The variation of both crack incidence and crack length may be expected to influence the measured mechanical properties of electrolytically deposited chromium.

2.3. *Mechanical properties*

2.3.1. Hardness measurements. The hardness of each sample was determined by averaging eight readings taken on each transverse section produced, using a Vicker's hardness tester with a load of 300 g. In each case the thickness of the deposit was approximately 200 μm. The results, which are summarized in Fig. 7 are the mean of all measurements taken on a minimum number of five specimens. The hardness is seen to be

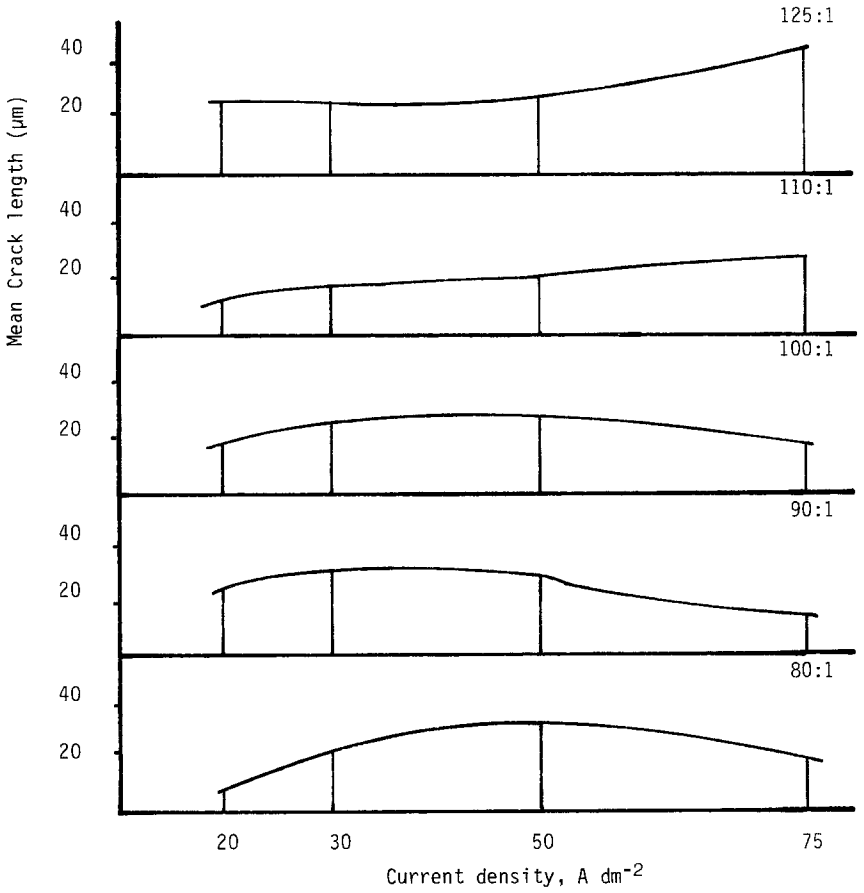

Fig. 5. Mean crack length versus current density for various sulphate ratios.

relatively insensitive to sulphate ratio, as shown in Fig. 7a, but changes appreciably with current density (Fig. 7b).

2.3.2. Tensile strength measurements. Initially, tubular samples were produced by simply plating onto a 15 mm copper tube. After dissolving away the copper the chromium tube was glued into suitable endcaps and tested on an Instron hard bed machine. This was found to be unsatisfactory as jaw fractures regularly occurred. An arrangement was then devised to produce shaped specimens in which the central area was produced at an accurately controlled density, while the end regions were formed under less controlled conditions. The results obtained for the sulphate ratios and current densities of interest are given in Table 2. All figures given are the average of a minimum of five specimens and the error bar varies from $\pm 20\%$ at $20\,A\,dm^{-2}$ (100:1 ratio) to $\pm 35\%$ at $75\,A\,dm^{-2}$ (110:1 ratio).

Table 2. Tensile strength of chromium tubes produced with variation of current density and $CrO_3 : H_2SO_4$ ratio. Process temperature 55° C

Current density ($A\,dm^{-2}$)	*Tensile strength ($kg\,cm^{-2}$)*				
	80:1	*90:1*	*100:1*	*110:1*	*125:1*
20	738	858	1579	34	109
30	719	330	652	100	250
50	637	372	515	215	178
75	303	334	430	259	293

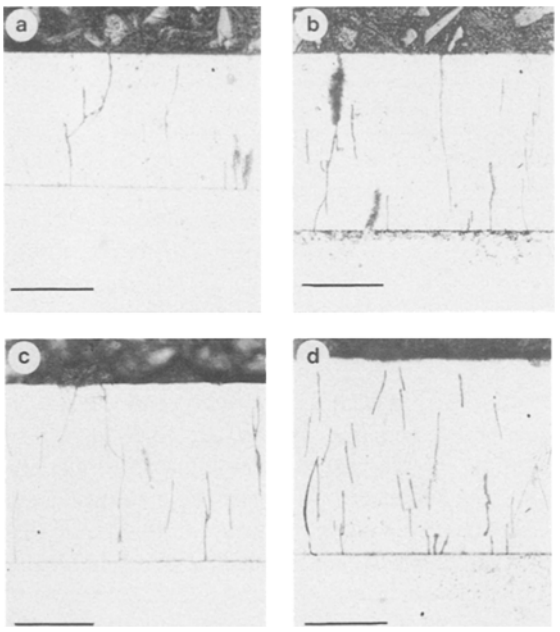

Fig. 6. Crack type in a solution with 100:1 sulphate ratio for various current densities: (a) 20 A dm^{-2}; (b) 30 A dm^{-2}; (c) 50 A dm^{-2}; (d) 75 A dm^{-2}. Scale bars: 47 μm.

As can be seen the highest average ultimate tensile strength (UTS) obtained corresponds to a test specimen plated at 20 A dm^{-2} in a 100:1 ratio CrO_3/H_2SO_4 solution. The UTS values obtained fall sharply either side of this sulphate ratio. Also, as the current density increases from 20 to 30 A dm^{-2} the UTS drops for sulphate ratios less than 100:1; this effect is very pronounced at 100:1 and 90:1, is insignificant at 80:1 and an increase occurs at higher ratios. The

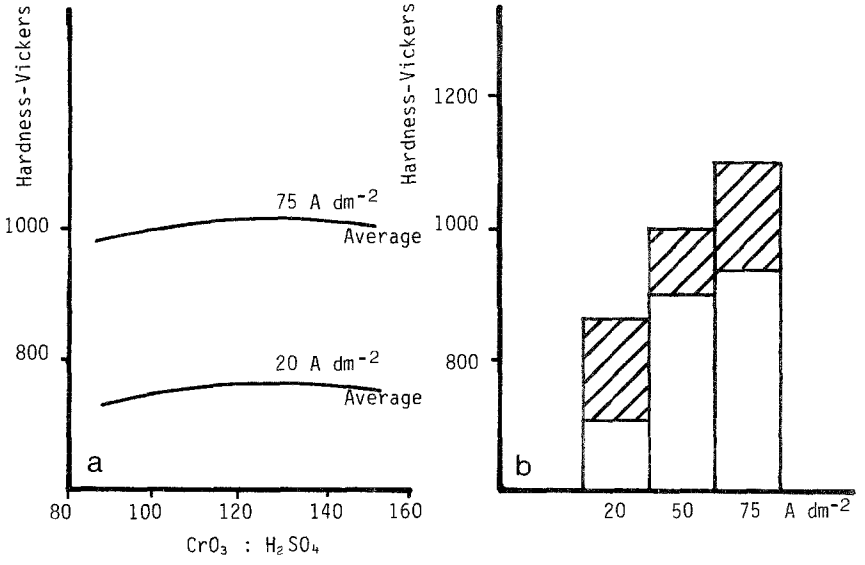

Fig. 7. (a) Variation of microhardness with electrolyte sulphate ratio. (b) Variation in microhardness with current density for a sulphate ratio of 100:1.

Table 3. Adhesion numbers (in Newtons) for electrodeposited chromium on mechanically polished and electropolished steel substrates with variation of current density and $CrO_3 : H_2SO_4$ ratio. Process temperature, 55° C

Current density ($A\,dm^{-2}$)	Mechanical polish					Electropolish				
	80 : 1	90 : 1	100 : 1	110 : 1	125 : 1	80 : 1	90 : 1	100 : 1	110 : 1	125 : 1
20	351	215	463	210	217	216	241	492	207	212
30	342	213	275	205	337	255	202	283	208	434
50	354	202	215	207	204	220	203	315	205	218
75	348	204	349	201	338	237	212	328	200	246

results obtained may best be explained by reference to Figs 3, 4 and 5 in terms of crack incidence and crack length. For example, where macrocracks predominate at high sulphate ratios (low crack incidence and large crack length), the UTS is low. This is seen in the results for 20 A dm^{-2} for ratios of 110 : 1 and 125 : 1. The rise in UTS with current density is consistent with increasing crack incidence and decreasing crack length, as evidenced in Figs 3 and 4.

Microcracked chromium gives higher values of UTS and improved apparent strength. The test in itself is very much a test of crack propagation under axial loading conditions, with the 20 A dm^{-2} 100 : 1 ratio case perhaps showing a tensile strength. Results gained by Chen and Baldauf [19] for low contractile chromium, which is not inherently cracked, are not masked by the effect of crack propagation.

2.3.3. Adhesion measurements. This test is an adaptation of an idea commonly used to measure the adhesion of thin vapour-deposited films [20] in which a stylus is drawn across a coating under a continuously or discretely increasing load. The load at which the film is torn away from the substrate is then taken as a measure of the film–substrate adhesion. In the case of chromium coatings the load at which the first coating to substrate failure is detected is used to indicate an adhesion strength.

The cutting tool used has disposable carbide tips which guarantees a constant tool profile in all tests. Following the test the specimen is sectioned and mounted for examination in a scanning electron microscope. The specimens are sequentially scanned and the first chrome–substrate failure is detected using the analysis facility. From each specimen six separate results were obtained and an average load at failure computed. The results obtained for both mechanically and electropolished specimens are given in Table 3. From the results no discernable difference between electropolished or mechanically polished specimens is evident except for sulphate ratios of 80 : 1. The best adhesion figures obtained are at 20 A dm^{-2} in a 100 : 1 solution, although at present no explanation can be given for this.

2.3.4. Stress measurements. The inherent stress in chromium deposits produced at varying current densities and temperatures was measured using a modified Hoare–Arrowsmith cell. Initial interface stress was not measured and as can be seen from Fig. 8 the final inherent stress in chromium coatings of greater than 10 μm is similar for all conditions. Also, increasing solution temperature drastically reduces initial stress, and at 85° C the final average stress condition is reached rapidly, for example within a coating thickness of 2 μm at 20 A dm^{-2} in a 100 : 1 solution.

3. Influence of current density upon coatings

A gun tube, 120 mm in length, was modelled, and for specified potential conditions imposed at the anode and cathode surfaces the potential gradient for the bounded problem was solved using the boundary element method. The resulting average current density distribution over the cathode surface (gun tube) is shown in Fig. 9. As can be seen, the current density in the chamber is some 10% greater than that in the barrel and at the barrel–chamber transition there is some variation. A more detailed study in this area

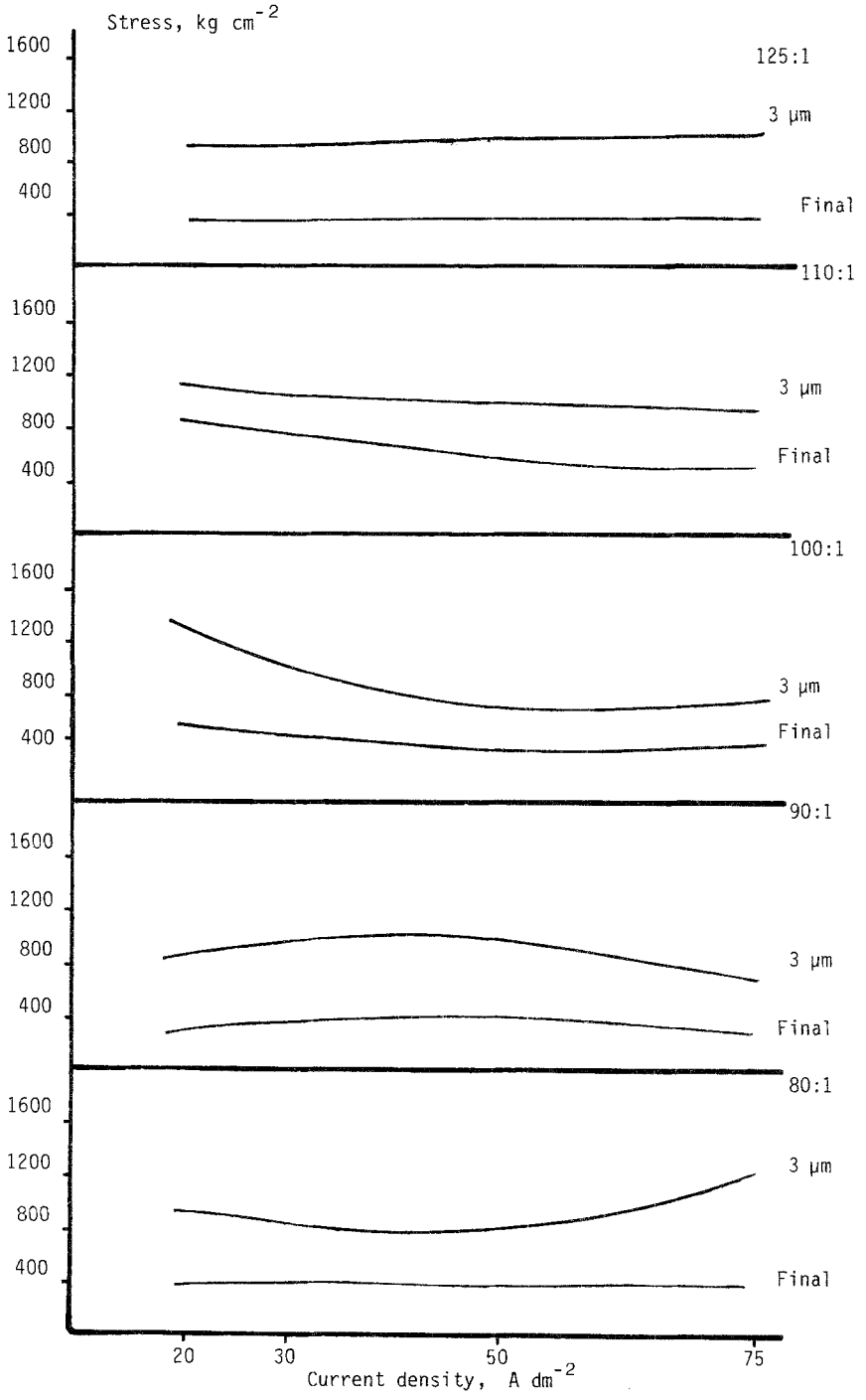

Fig. 8. Internal stress as a function of current density for electrodeposited chromium at various ratios. Separate curves shown for stress at a thickness of 3 μm and for a final stress level.

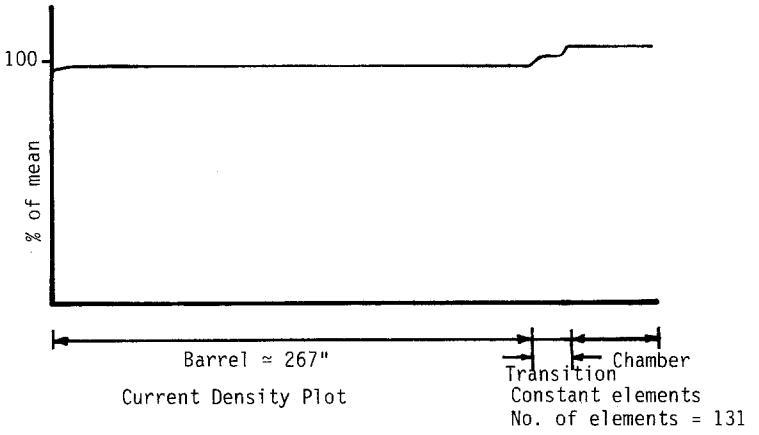

Fig. 9. Current density distribution over the gun tube length as a percentage of mean.

shows that the current variations are not significant so far as deposit structure is concerned (Fig. 10). However, it is to be expected that a significant variation will exist between the land and groove in the barrel itself, typically 2:1. This is shown to be the case in Fig. 11. The consequence of such a low current density in the groove region as seen from Figs 3 and 5 is a high crack incidence with low crack length.

Examination of a gun tube plated in a 250 $g\,l^{-1}$ chromic acid solution, with a chromic to sulphuric acid ratio nominally controlled between 90:1 to 110:1, shows a chromium structure relatively insensitive to current density

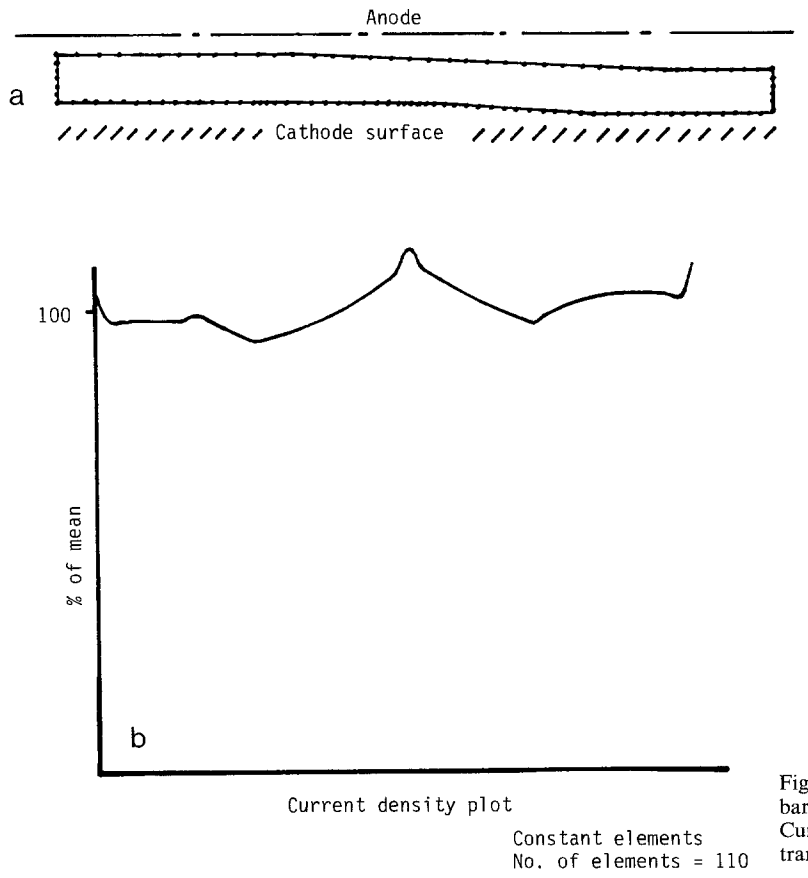

Fig. 10. (a) Boundary element model in barrel–chamber transition area. (b) Current variation in barrel–chamber transition area.

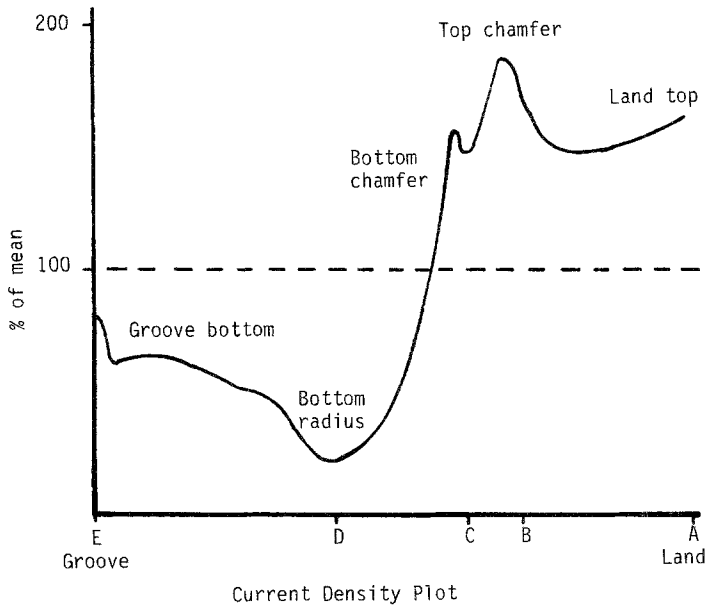

Fig. 11. Current variation over land and groove in rifled section.

in areas of high current density as shown in Fig. 12. However, in the area where the current density is very much less than 20 A dm^{-2} a high crack incidence, low crack length structure is observed, as predicted (Fig. 13).

The results obtained show that the laboratory-based results are applicable to the full-scale plating situation.

4. Conclusions

It has been shown, as expected, that both sulphate ratio and current density affect the structural characteristics of chromium plate. As current density conditions vary in a gun tube, especially in the barrel, the chromium coating will not be homogeneous; however, in 100:1 solutions above 30 A dm^{-2} the crack incidence and crack length are relatively constant. This is shown to be the case in a production barrel.

From the mechanical test results both tensile strength and adhesion are maximum at a lower current density, although both are probably influenced by the crack pattern. Deposit hardness is sensitive to current density but insensitive to sulphate ratio, and to date no evidence exists which suggests hardness to be an important parameter. Stress in the deposit may influence the crack pattern observed, but final stress is approximately constant and is related to the inherent

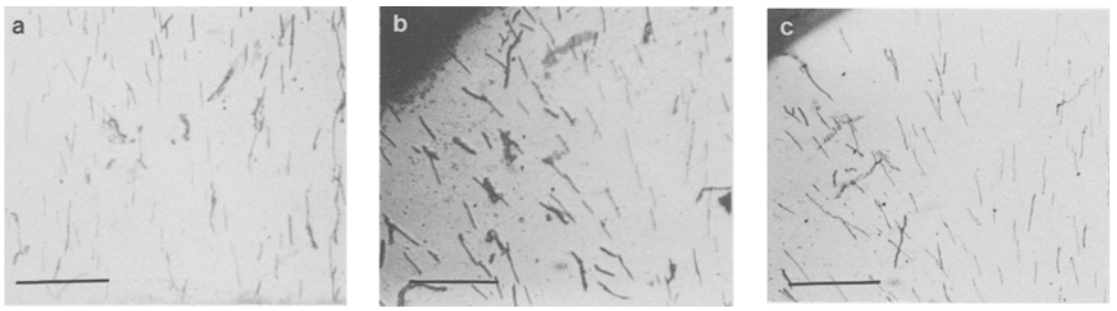

Fig. 12. Structure of chromium at commencement of rifling and top edge of land chamfer. (a) Land top; (b) top edge chamfer; (c) lower edge chamfer. Scale bars: 57 μm.

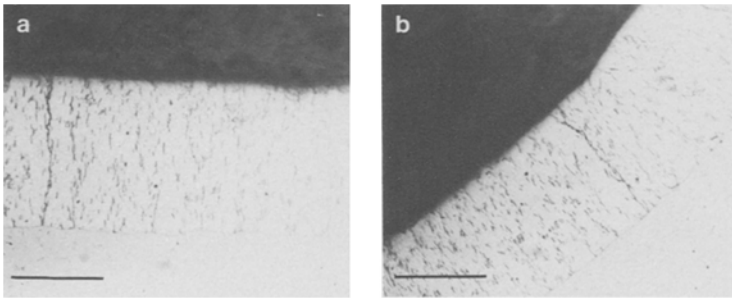

Fig. 13. Structure of chromium in groove bottom (a) and at bottom radius (b) after commencement of rifling. Scale bars: 57 μm.

strength of the chromium. Coatings produced at high temperatures (85°C) in any solution tested achieve this final value at a deposit thickness of less than 2 μm. Also, in all situations the initial coating stress is reduced with increasing current densities.

Although an information base for sulphate-catalysed solutions operating over a range of temperatures and current densities has been established, no in-service test results have been obtained to establish the most appropriate coating characteristics for gun tube applications. However, it has been shown that the laboratory results obtained are applicable to the practical plating situation. This should eventually result in the upgrading of the high contractile chromium coating process in conventional plants.

Acknowledgements

This work has been carried out with funding provided by the Ministry of Defence, and both authors wish to express their indebtedness to Mr A. R. Sheward (RARDE) for his support.

References

[1] N. E. Ryan, *Met. Finish.* **62** (1965) 46.
[2] F. A. Lowenheim, 'Electroplating', McGraw-Hill, New York (1978).
[3] J. L. Griffin, *Plating* **53** (1966) 196.
[4] J. P. Hoare, *J. Electrochem. Soc.* **126** (1979) 190.
[5] R. L. Sass and S. L. Ascher, *Plating* **41** (1954) 497.
[6] D. Reinskonwski and C. A. Knorr, *Z. Elektrochem.* **58** (1954) 709.
[7] R. Weiner, *Met. Finish.* **64** (1966) 46.
[8] E. Leibricht, *J. Electrochem.* **33** (1927) 69.
[9] *Idem, Trans. Faraday Soc.* **31** (1935) 1188.
[10] J. Lin-Cai and D. Pletcher, *J. Appl. Electrochem.* **13** (1983) 235.
[11] *Idem, ibid.* **13** (1983) 245.
[12] US Patent, 4450050 (1984).
[13] M. A. Shluger, *Russian Eng. J.* **54** (1974) 72.
[14] UK Provisional Patent, 84110.63 (1984).
[15] J. C. Saiddington and G. R. Hoey *J. Electrochem. Soc.* **117** (1970) 1011.
[16] C. A. Snavely and C. L. Faust, *ibid* . **97** (1950) 99.
[17] M. McCormick, S. Y. S. Parn and D. Howe, AIChemE Annual Conference, Cleveland, Ohio (1983). Microfiche: paper 10e.
[18] S. Y. S. Parn, M. McCormick and D. Howe, *Trans. IMF* **59** (1981) 61.
[19] E. S. Chen and W. Baldauf, US Army Research and Development Command, Report No. ARLCB-TR-80008.
[20] H. K. Pulker, A. J. Perry and R. Berger, *Surf. Technol.* **14** (1981) 25.